This article has been accepted for publication in a future issue of this journal, but has not been fully edited. Content may change prior to final publication. Citation information: DOI 10.1109/JBHI.2015.2450196, IEEE Journal of Biomedical and Health Informatics

The Removal of EOG Artifacts from EEG Signals Using Independent Component Analysis and Multivariate Empirical Mode Decomposition

Gang Wang*, *Member, IEEE*, Chaolin Teng, Kuo Li, Zhonglin Zhang, Xiangguo Yan

***Abstract*—The recorded electroencephalography (EEG) signals are usually contaminated by electrooculography (EOG) artifacts. In this paper, by using independent component analysis (ICA) and multivariate empirical mode decomposition (MEMD), the ICA-based MEMD (IMEMD) method was proposed to remove EOG artifacts (EOAs) from multichannel EEG signals. Firstly, the EEG signals were decomposed by the MEMD into multiple multivariate intrinsic mode functions (MIMFs). The EOG-related components were then extracted by reconstructing the MIMFs corresponding to EOAs. After performing the ICA of EOG-related signals, the EOG-linked independent components (ICs) were distinguished and rejected. Finally, the clean EEG signals were reconstructed by implementing the inverse transform of ICA and MEMD. The results of simulated and real data suggested that the proposed method could successfully eliminate EOAs from EEG signals and preserve useful EEG information with little loss. By comparing with other existing techniques, the proposed method achieved much improvement in terms of the increase of signal-to-noise (SNR) and the decrease of mean square error (MSE) after removing EOAs.**

***Index Terms*—EEG, EOG artifacts, multivariate empirical mode decomposition, ICA**

I. Introduction

ELECTROENCEPHALOGRAPHY (EEG) can be recorded from the scalp of human head by suitable electrodes and reflect the important information about brain electrical activity. Due to its convenient acquisition, noninvasive access, and high temporal resolution, EEG signals play an increasingly important role in the field of cognitive research, disease diagnosis, and rehabilitation engineering [1-4]. These signals have small amplitudes and strong randomness, so they can be very easily contaminated with various artifacts. One of the most common artifacts influencing the quality of EEG signals are the electrooculography (EOG) activities whose magnitude is usually much higher than that of EEG signals. EOG has a burst of high-energy in low-frequency, which seriously affects the EEG basic rhythm waves, like δ waves (0.5 - 4Hz) and θ waves (4 - 8Hz) [5]. EOG artifacts (EOAs) can make the analysis and interpretation of EEG signals difficult and will also affect the diagnosis of doctors. In order to reduce the interference of EOAs, subjects are asked not to blink for a long time or to blink as infrequently as possible, which causes eyes discomfortable. Especially for some specific patients, such as children with attention deficit hyperactivity disorder (ADHD), it is difficult to obey it. Hence, many EOAs often appear in EEG signals. The common clinical practice is to directly reject EEG segments with eye artifacts. However, it may lead to some loss of important EEG information. Therefore, it is very essential to effectively remove EOAs from EEG signals and preserve underlying brain activity signals with little distortion in the preprocessing of EEG signals.

Many attempts are made to remove various artifacts from EEG signals. Traditional filters work well to eliminate electrical line noise and other high-frequency artifacts. However, EOAs have a spectral overlap with underlying EEG signals. Therefore, the filter-based EOG removal can result in the loss of EEG information [6]. For the ocular artifact correction method based on regression in the time domain, because there is a cross-interference between EOG and EEG, these two kinds of signals can be influenced by each other. Thus, the EOAs may be overestimated and some useful EEG components can be lost in the corrected EEG signals [7]. Recently, Jung et al. apply the independent component analysis (ICA) method to decomposing EEG signals into multiple independent components (ICs). Then, the EOG-linked ICs are rejected by EEG waveforms and EEG topography maps [8]. Nevertheless, the directed removal of the artifact-linked IC may cause the loss of EEG information and is unsuitable for real-time applications. Kelly et al. indicate that the thresholding adaptation method based on discrete wavelet transform (DWT) produce superior reduction of ocular artifacts [9]. Peng et al. combine DWT and adaptive noise cancellation for the removal of ocular artifacts in portable application [10]. Subsequently, some investigators introduce the techniques based on the combination of wavelet transform and ICA for suppression of EOAs in EEG recordings [11-13]. Additionally, empirical mode decomposition (EMD) is an adaptive method for analyzing the nonlinear signal [14-16]. Many EMD-based methods are proposed to remove EOAs. Lindsen et al. combine the ICA and the EMD for correction of blink artifacts [17]. Zeng et al. employ the stationary subspace analysis (SSA) and

Manuscript received December 31, 2014. This work was supported by the National Natural Science Foundation of China under Grant no. 81201162, no. 61471291, the Natural Science Basic Research Plan in Shaanxi Province of China under Grant No. 2013JQ8007, and the Fundamental Research Funds for the Central Universities of China. *Asterisk indicates corresponding author.*

*G. Wang, C. Teng and X. Yan are with the Key Laboratory of Biomedical Information Engineering of Ministry of Education, Institute of Biomedical Engineering, School of Life Science and Technology, Xi'an Jiaotong University, Xi'an, 710049, China (e-mail: ggwang@mail.xjtu.edu.cn).

K. Li and Z. Zhang are with the Department of Neurosurgery, First Affiliated Hospital, Xi'an Jiaotong University, Xi'an, 710061, China.

This article has been accepted for publication in a future issue of this journal, but has not been fully edited. Content may change prior to final publication. Citation information: DOI 10.1109/JBHI.2015.2450196, IEEE Journal of Biomedical and Health Informatics

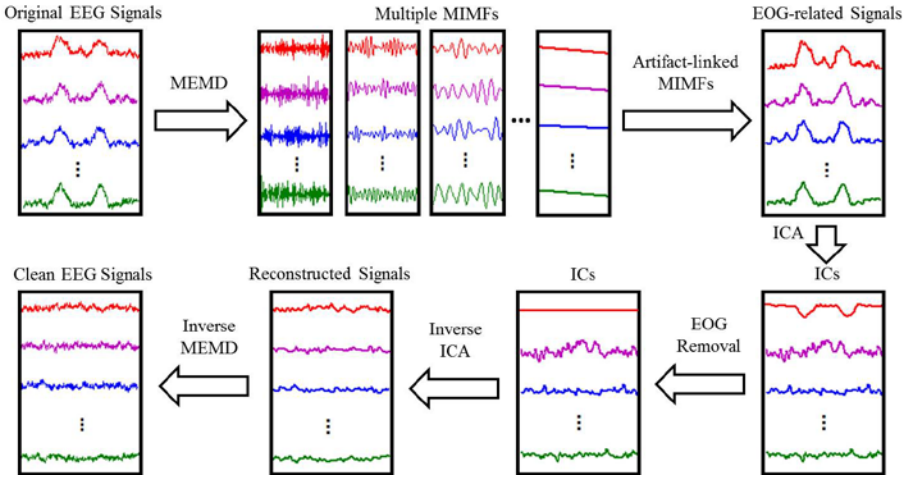

Fig. 1. The algorithm flowchart of the IMEMD method proposed in this study.

the EMD for EOA artifact correction [18]. More recently, by using the multivariate empirical mode decomposition (MEMD), the EOG-related components can be separated from the EEG signals [19]. However, this method loses much EEG information after the rejection of EOAs.

In this study, a novel ICA-based MEMD (IMEMD) method was proposed to improve the performance of removing EOAs from multichannel EEG signals. The results from simulated and real data showed that the proposed method could successfully remove EOAs while useful EEG signals were preserved with little information loss. In order to further verify the effectiveness of proposed method, the IMEMD technique was compared with other existing methods. It was demonstrated that the proposed method achieved much improvement in terms of removing EOAs and preserving EEG information.

II. METHODS

A. Analysis Paradigm

As depicted in the algorithm flowchart of Fig. 1, the proposed IMEMD method consists of five steps. Firstly, the MEMD technique was used to decompose multichannel EEG signals into multiple multivariate intrinsic mode functions (MIMFs). Secondly, the MIMFs related to EOAs were selected to reconstruct EOG-related signals while the other MIMFs were retained. Thirdly, multiple independent components (ICs) were obtained by ICA for the EOG-related signals. Fourthly, EOG-linked ICs were distinguished and rejected. Finally, by performing the inverse transform of ICA and MEMD, the clean EEG signals without EOAs were reconstructed. According to the sequence of the block diagram of IMEMD algorithm, the detailed approach can be described as follow.

1) Multivariate Empirical Mode Decomposition: It is well-known that the EMD method can only deal with one-dimensional signals. As the extension of EMD method, MEMD can be used to handle the multiple-dimensional signals [20]. The MEMD algorithm can generate multiple n-dimensional envelopes by projecting the n-dimensional signal along different directions in n-dimensional spaces. Then, local mean can be obtained by averaging all n-dimensional envelopes. In order to extract MIMFs, the difference is calculated by subtracting local mean from original signal. If the difference fulfills the stoppage criteria, it can be regarded as first MIMF. After extracting first MIMF, the difference between first MIMF and original signal is defined as a new signal to extract next MIMF. When the extracted signal meets the stoppage criteria of MEMD, the whole decomposition process is finished. In this study, given that $x(t) = (x_1(t), x_2(t), ..., x_n(t))^T$ is a n-channel EEG signal and $e(t)$ is one-dimensional EOG reference signal, $x(t)$ can be decomposed by using MEMD as $x(t) = \sum_{i=1}^{i=m} MIMF_i(t)$, where $MIMF_i(t)$ is the *ith* MIMF. Because the amplitudes of real EOG signals were greater than those of EEG signals, the channel with maximum amplitude was chose from EEG signals as the EOG reference.

2) Artifact-linked MIMFs Selection: EOAs are characterized by abnormal burst of high-energy in low-frequency. Time-frequency evolution pattern of EOAs is observable in artifact-contaminated EEG recordings. Therefore, the time-frequency similarity between two signals was used for the selection of artifact-linked MIMFs. Because the spectrum of EOAs is often concentrated in the frequencies below 10 Hz [5], the time-frequency representation (TFR) of EOG reference between 0 and 10 Hz was computed by using wavelet transformation. For each MIMF, the TFR between 0 and 10 Hz was also obtained by averaging the wavelet transformation of all channels of signals. Then, the correlation coefficients between EOG-TFR and each MIMF-TRF were calculated. Because the frequency bands of MIMFs were ranked from high frequency to low frequency, correlation coefficients were sorted ascendingly. The critical MIMF was determined by searching the maximum difference between adjacent correlation coefficients. If the *jth* MIMF satisfied the above condition, the EOG-related signal could be calculated by summing all artifact-linked MIMFs, which was denoted by $u(t) = \sum_{i=j}^{i=m} MIMF_i(t)$. At the same time, the retained EEG signal without EOAs was obtained by other MIMFs, namely $v(t) = \sum_{i=1}^{i=j-1} MIMF_i(t)$. Additionally, visual inspections were

This article has been accepted for publication in a future issue of this journal, but has not been fully edited. Content may change prior to final publication. Citation information: DOI 10.1109/JBHI.2015.2450196, IEEE Journal of Biomedical and Health Informatics

used to assist the selection of artifact-linked MIMFs.

3) Independent Component Analysis: ICA was firstly proposed in 1994 by Comon, aiming to solve the blind source separation problem [21]. The basic idea of ICA algorithm is to decompose the observed signals into several ICs according to the principle of statistical independence. In this study, the EOAs can be eliminated by separating EOG from EEG signals by using ICA because EOG and EEG generated by different sources are independent each other. The EOG-related signal $u(t)$ was then decomposed by the ICA to obtain multiple ICs.

4) EOG-linked ICs Selection: After the EOG-related signal $u(t)$ was analyzed by the ICA method, the EOG-linked ICs should be recognized because not all ICs included EOAs. Here the fourth-order cumulant (kurtosis) was used to recognize the EOG-linked ICs due to its computational and theoretical simplicity [22]. Given a one-dimensional random variable x, the kurtosis can be defined as $k = m_4 - 3m_2^2$, where $m_n = E\{(x-m_1)^n\}$ is the nth order central moment of random variable, and m_1 is the mean value of variable. The kurtosis is negative for a sub-Gaussian random signal and zero for a Gaussian signal such as clean EEG signals, but it is positive for super-Gaussian distributions of peaked activities such as eye blink and cardiac artifacts [22]. Therefore, an appropriate threshold of kurtosis can be employed to discriminate EOAs. In this study, the kurtosis of each IC was estimated and these values were normalized to avoid the effect of different amplitude scales on the following calculation. Specifically, the kurtosis values of all ICs were normalized to center it at zero mean and scale it to unit standard deviation. Because the kurtosis had been normalized according to all ICs, the determination of kurtosis threshold was independent on different dataset and the practical value of threshold could be selected by trial and error. The critical threshold value was set at 1.5 in this paper [12, 23]. Finally, the ICs whose normalized kurtosis values were greater than the threshold value were automatically detected as EOG components and were assigned as zero values.

5) Signal Reconstruction: The EOAs was represented by the EOG-linked ICs. After the EOG-linked ICs were removed, the remaining ICs were back-projected to the set of artifact-free components. Subsequently, the EOG-free signals $u'(t)$ could be obtained by applying the inverse transform of ICA to the artifact-free components. Finally, the clean EEG signals were reconstructed by summing the EOG-free signals $u'(t)$ and the retained signals $v(t)$ according to the inverse transform of MEMD.

B. Quantitative Validation Measures

After the removal of EOAs, signal-to-noise (SNR), mean square error (MSE) and cross-correlation coefficient (CRC) were regarded as the assessment criteria to quantitatively evaluate the performance of proposed method. The SNR of EEG can be defined as $SNR = 10*\lg(\sum_{i=1}^{n} x_i^2 \Big/ \sum_{i=1}^{n} y_i^2)$, where x_i denotes pure EEG signal, y_i represents artifacts calculated by subtracting pure EEG signals from clean EEG signals, and n is the total number of samples before the removal of EOAs [24]. The mean SNR can be obtained by averaging the values corresponding to all channels of EEG signals. The larger the value of SNR is, the less the noise contained in the mixed signal is. Thus, the SNR can be employed to describe the removal degree of EOAs from EEG signals.

The value of MSE indicates the degree of similarity between two signals. The MSE of signals can be calculated by $MSE = \frac{1}{n}\sum_{i=1}^{n}(x_i - y_i)^2$, where x_i denote pure EEG signals, y_i represent mixed EEG signals, and n is the total number of samples [25]. The smaller the value of MSE is, the higher the similarity degree between two signals is. Therefore, the MSE can be used to measure the reserved degree of EEG information after rejecting EOAs.

The value of CRC represents the correlation degree between two signals. Because the CRC between two signals with opposite polarity is a negative value, the absolute value of CRC is used in this study. The smaller the absolute value of CRC is, the lower the degree of linear correlation between two signals is. When the CRC value is approximately equal to zero, there is no linear correlation between two signals. It is generally considered that the CRC value between EEG and EOG should be greater than 0.4 before removing EOAs and the CRC should be less than 0.4 after EOAs rejection [26]. As such, the CRC between EEG and EOG can be utilized to judge whether EOAs are removed or not. The CRC between two signals can be denoted by [26]:

$$CRC = \frac{\left|\sum_{i=1}^{n}(X_i - \overline{X}) * \sum_{i=1}^{n}(Y_i - \overline{Y})\right|}{\sqrt{\sum_{i=1}^{n}(X_i - \overline{X})^2} * \sqrt{\sum_{i=1}^{n}(Y_i - \overline{Y})^2}} \quad (1)$$

where X and Y represent two kinds of signals, and n is the total number of samples.

C. Description of Simulated EEG Data

Both EEG and EOG signals were obtained in the MATLAB platform. The sampling rate of signals was set at 200Hz. Ninety groups of pure EEG signals were generated by the noise.m function [27] and each group data was represented by the matrix A (size: 5×1600). One group of simulated EOG was generated by the peak.m function [28] and the simulated EOA was denoted by the matrix B (size: 5×1600). The artifact-contaminated EEG signals can be achieved by mixing matrix A with matrix B in the following manner [29]:

$$C(i,:) = A(i,:) + \lambda * B(i,:), i \in \{1,2,3,4,5\} \quad (2)$$

where matrix C is the simulated EEG signals included EOAs, and λ is a scale coefficient. By changing the value of λ, EEG and EOG were mixed together in the case of different SNRs with -15dB, -10dB, -5dB, and 0dB. For each SNR, 90 groups of artifact-contaminated EEG signals were generated in this simulation.

This article has been accepted for publication in a future issue of this journal, but has not been fully edited. Content may change prior to final publication. Citation information: DOI 10.1109/JBHI.2015.2450196, IEEE Journal of Biomedical and Health Informatics

D. Real EEG Data Acquisition

To further validate the feasibility and effective of the proposed method, the performance of IMEMD was verified by using real EEG signals. Three healthy human subjects (males, mean age 23, range 22-24 years old) voluntarily accepted to take part in this study. Written informed consent approved by the institutional review board at Xi'an Jiaotong University was obtained from the subjects before the experiments. The scalp EEG data were recorded with a SynAmps2 amplifier (Neuroscan Systems, Compumedics, Charlotte, NC, USA) from 32 scalp electrodes placed according to the standard 10–20 system. The channel Cz at the top of the head was used as the reference electrode. Differential amplifiers with band-pass filters between 0.1 and 100 Hz were used to minimize the effects of high frequency noise and low frequency artifacts. The sampling frequency of signals was 500 Hz. Thirty EEG segments contaminated by EOAs were cut off from each subject and the length of EEG segments ranged from 3 to 8 s. Subsequently, the first five channels of each segment with obvious EOAs and the EOG reference channel were selected to perform EOAs rejection by using the proposed method.

III. RESULTS

A. Removing EOAs from Simulated EEG Signals

The IMEMD method was used to reject EOAs from 90 groups of artifact-contaminated EEG signals when the SNR of original EEG signals was 0dB. In this study, four kinds of ICA algorithms were used: maximum likelihood (ML) algorithm, joint approximate diagonalization (JADE) algorithm, fast ICA algorithm, and extended-informax algorithm. These ICA-based MEMD methods were denoted by MMEMD, JMEMD, FMEMD, and EMEMD, respectively. Fig. 2 illustrates the discrimination of SNRs and MSEs after the rejection of EOAs among four kinds of methods for the SNR of original artifact-contaminated EEG signals with 0dB. The mean and standard deviation values of SNRs and MSEs after performing EOAs removal were calculated by using 90 realizations of the simulated EEG signals for each EEG channel. On one hand, the proposed method achieved obvious performance enhancement in terms of SNR after EOAs removal. This indicated that the EOAs have been effectively removed from the original EEG signals. Furthermore, because the MMEMD method resulted in higher SNR after EOAs removal than other three methods, the MMEMD approach removed the most EOAs among four kinds of method. On the other hand, the MSE of each channel of EEG signals had been obviously reduced after EOAs removal. This demonstrated that the majority of EEG information was preserved after the removal of EOAs. As shown in Fig. 2, the MSE obtained by the MMEMD method was less than other methods, so the MMEMD method reserved the most useful EEG information among four kinds of method. Moreover, by comparing the EEG waveforms before and after EOAs removal, it could be observed that the EOAs were successfully eliminated from the artifact-contaminated EEG signals. According to the experimental results of different IMEMD algorithms, because the MMEMD approach was superior to other methods, this method was employed to remove EOAs in the following calculation.

In addition to the performance evaluation based on different ICA algorithms, the automated wavelet ICA (AWICA) approach was also applied to removing EOAs from the original EEG signals [12]. The same EEG dataset was used in this comparison. Firstly, the mixed signals were decomposed into different EEG rhythms or wavelet components by discrete wavelet transform (DWT). Then, for the artifactual wavelet components which were selected automatically according to kurtosis and Renyi's entropy, the wavelet independent components were extracted by ICA algorithm. The wavelet independent components whose kurtosis or Renyi's entropy was greater than the threshold were regarded as the artifactual components and were assigned as zero. Finally, the clean EEG signals without EOAs were reconstructed by the inverse transform of ICA and DWT. Fig. 3 shows the numerical distinctions of SNRs of clean EEG signals after removing EOAs between the IMEMD method and the AWICA method for different SNRs of original EEG signals with -15dB, -10dB,

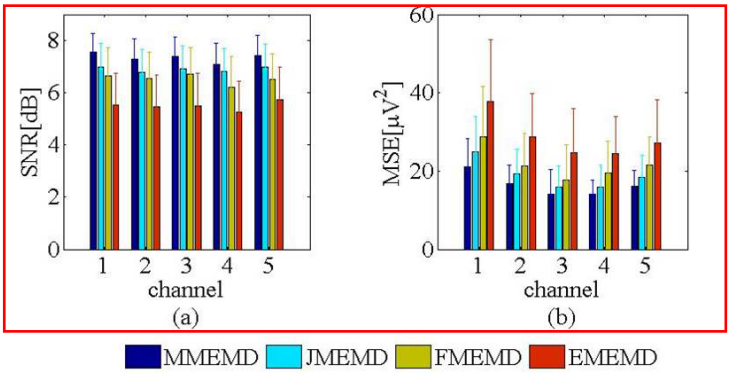

Fig. 2. Distinctions of SNRs and MSEs after EOAs rejection using the MMEMD method, the JMEMD method, the FMEMD method, and the EMEMD method when the SNR of original artifact-contaminated EEG signals was 0dB. Mean values corresponding to different methods are represented by different color bars. Short bars: standard deviations.

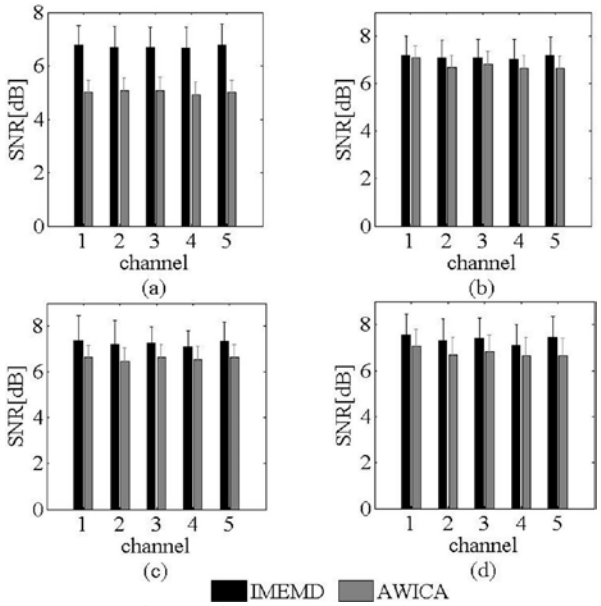

Fig. 3. Comparison of SNRs of clean EEG signals after EOAs removal using the proposed method and the AWICA method. The SNRs of original artifact-contaminated EEG signals are -15dB (a), -10dB (b), -5dB (c), and 0dB (d). Mean values corresponding to different methods are represented by different color bars. Short bars: standard deviations.

This article has been accepted for publication in a future issue of this journal, but has not been fully edited. Content may change prior to final publication. Citation information: DOI 10.1109/JBHI.2015.2450196, IEEE Journal of Biomedical and Health Informatics

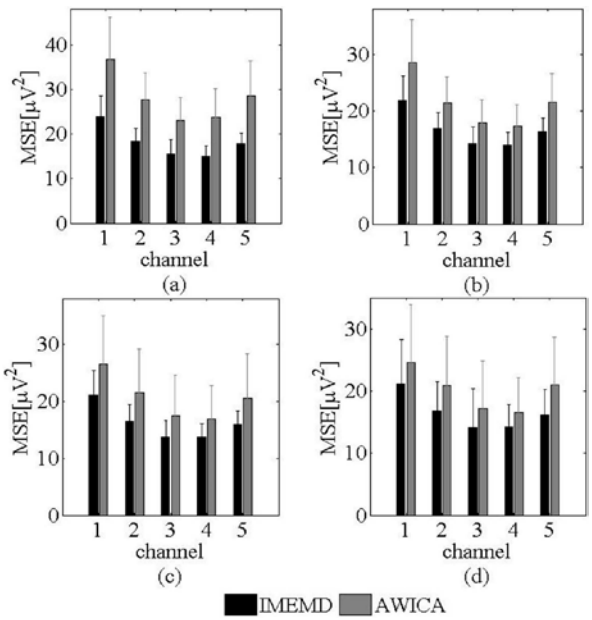

Fig. 4. Comparison of MSEs of clean EEG signals after EOAs removal using the proposed method and the AWICA method. The SNRs of original artifact-contaminated EEG signals are -15dB (a), -10dB (b), -5dB (c), and 0dB (d). Mean values corresponding to different methods are represented by different color bars. Short bars: standard deviations.

-5dB, and 0dB. The experimental results were also computed by 90 realizations of simulation EEG signals. It could be observed from this figure that the increase of SNR using IMEMD was superior when compared to that using AWICA for all EEG channels and original SNRs. When using the IMEMD approach, the averaged SNRs of clean EEG signals ranged from 6.65dB to 7.55dB. In terms of the AWICA approach, the averaged SNRs were between4.93dB to 7.08dB. Additionally, there was little influence of the original SNR on the performance of the IMEMD method. However, the denoising performance of AWICA method would descend markedly while the original SNR was deceased. Fig. 4 illustrates the MSE differences after removing EOAs between the IMEMD method and the AWICA method for different SNRs of original EEG signals with -15dB, -10dB, -5dB, and 0dB. As indicated in this figure, the decrease of MSE using IMEMD was more than that using AWICA for all EEG channels and original SNRs. Generally speaking, the MEMD is data-driven method whose decomposition basis is adaptively derived from the experimental data rather than assigned manually according to a priori knowledge of the signal component. Consequently, the MEMD is superior to other signals processing method such as Fourier and wavelet transformation [20, 30, 31]. Moreover, it is demonstrated that the MEMD is clearly suitable for processing non-deterministic and non-stationary electrophysiological signals because the MIMFs decomposed by MEMD can reflect the local characteristics of signal at any time [32]. Thus, the IMEMD method can provide better validation measures than the AWICA method for the removal of EOAs.

B. Denoising Real EEG Data

In this study, the IMEMD method was employed to remove EOAs from real EEG signals. A typical multichannel of real EEG signals contaminated with eye blinks and the clean EEG signals after EOAs removal are illustrated in Fig. 5. As shown in Fig. 5 (a), each EEG channel was influenced by eye blinks before removing EOAs. Especially, the first several channels included the large amplitude of obvious ocular artifacts. The last channel denotes EOG reference. After signal denoising, it could be found that the EOAs were almost removed from the artifact-contaminated EEG signals. Because both EEG and EOG were unknown in original EEG signals, SNR and MSE would not be regarded as the evaluation criteria of artifact removal. However, the CRC values between EEG and EOG could be employed to determine whether EOAs were removed or not. The quantitative differences of CRC values before and after removing EOAs for three subjects are shown in Table I. The mean and standard deviation of CRC values were calculated by using 30 realizations of EEG signals for each individual EEG channel. It could be observed that the CRC values between EEG and EOG reference were greater than 0.4 before EOAs removal. Particularly, the CRC values between several EEG channels and EOG reference were close to 1, which indicated that these two signals had significant linear correlation. After rejecting EOAs, the correlation degree between EEG and EOG was obviously reduced since the CRC values were less than 0.4. By using the one-way analysis of variance (ANOVA), there were significant differences between the CRC values before and after EOAs removal. Additionally,

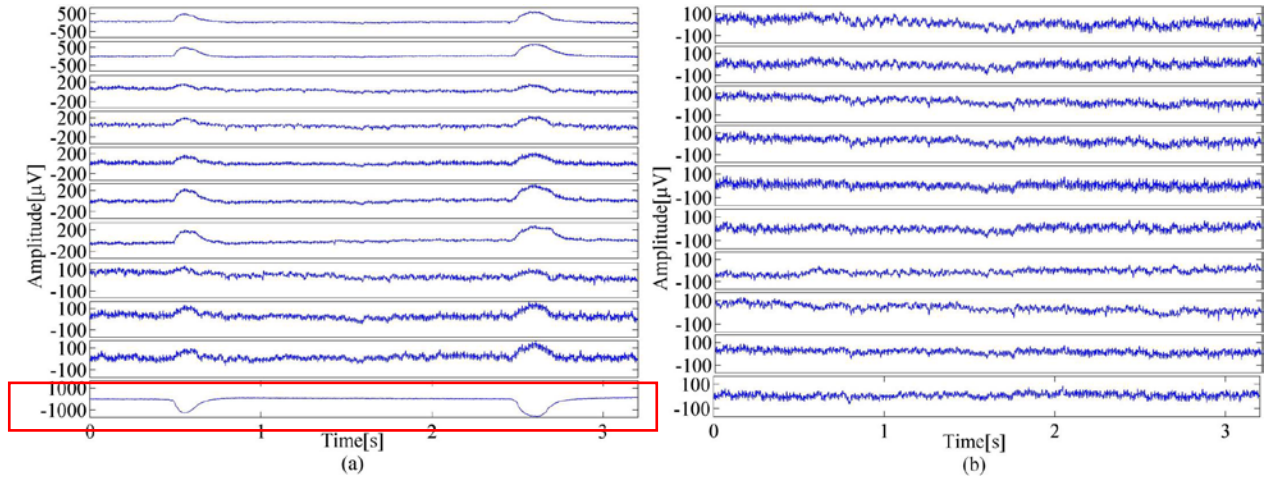

Fig. 5. (a) A typical example of real EEG signals contaminated with eye blinks, where the last channel represents EOG reference channel. (b) The multichannel of artifact-free EEG signals after the EOAs removal.

This article has been accepted for publication in a future issue of this journal, but has not been fully edited. Content may change prior to final publication. Citation information: DOI 10.1109/JBHI.2015.2450196, IEEE Journal of Biomedical and Health Informatics

TABLE I
CROSS-CORRELATION COEFFICIENTS BEFORE AND AFTER EOAS REMOVAL BY USING THE PROPOSED METHOD

EEG Channel			FP1	FP2	F7	F3	F2	F4	F8	FT7	FC3	FCz
CRC	S1	Before	0.96±0.02	0.98±0.01	0.71±0.12	0.81±0.07	0.80±0.07	0.92±0.03	0.89±0.06	0.55±0.13	0.66±0.12	0.61±0.13
		After	0.20±0.12	0.18±0.13	0.15±0.11	0.15±0.11	0.08±0.06	0.16±0.11	0.21±0.13	0.17±0.12	0.20±0.10	0.15±0.12
	S2	Before	0.97±0.03	0.77±0.25	0.81±0.17	0.85±0.12	0.80±0.13	0.73±0.16	0.44±0.24	0.72±0.20	0.75±0.19	0.63±0.17
		After	0.25±0.09	0.14±0.11	0.19±0.11	0.18±0.12	0.19±0.08	0.18±0.11	0.18±0.10	0.20±0.12	0.19±0.10	0.16±0.10
	S3	Before	0.94±0.04	0.96±0.03	0.78±0.14	0.85±0.07	0.71±0.11	0.87±0.04	0.83±0.09	0.67±0.15	0.69±0.14	0.65±0.14
		After	026±0.07	0.18±0.11	0.11±0.08	0.10±0.08	0.18±0.11	0.16±0.10	0.19±0.10	0.10±0.08	0.10±0.08	0.12±0.10

by comparing the EEG waveforms before and after EOAs removal, it could be found that the EOAs have been effectively removed from original artifact-contaminated EEG signals.

IV. DISCUSSION

It is inevitable to contain EOAs in the collected EEG signals during various experiments. As a common interference, the EOG makes further processing and analysis of EEG signals very difficult. In this study, by combining ICA and MEMD, the IMEMD method was proposed for the removal of EOAs. The EOG-related components were firstly extracted by reconstructing the MIMFs corresponding to EOAs. Then, after performing the ICA of EOG-related signals, the EOG-linked ICs were distinguished and rejected by an appropriate threshold of kurtosis. Finally, the clean EEG signals were obtained by performing the inverse transform of ICA and MEMD. The results demonstrated that the EOAs were successfully suppressed and the EEG information was reserved to the greatest extent. This reveals that the proposed method is indeed an effective method for removing ocular artifacts.

In order to further discuss the performance of the proposed method, we compared this method with other existing algorithm. The combination of SSA and EMD (SSA-EMD) was employed in this comparison task [18]. To facilitate the effectiveness comparison, the same EEG dataset was applied to this method. Firstly, by applying SSA, the raw EEG data was divided into the cerebral activity and the highly non-stationary EOG components. Secondly, the EOAs were reconstructed from the identified EOG components by EMD algorithm. Finally, the EOAs were projected back to be subtracted from raw EEG signals to obtain the clean EEG signals. The SNR differences between the IMEMD method and the SSA-EMD method after performing EOAs removal are shown in Fig. 6. The comparison of MSEs between the IMEMD method and the SSA-EMD method after performing EOAs removal are shown in Fig. 7. From these two figures, it could be observed that the proposed method was better than the SSA-EMD method with regard to the improvement of SNR and MSE after removing EOAs. The EMD method can adaptively decompose the original signal into a finite set of band-limited signal oscillators termed as intrinsic mode functions (IMFs) [14]. This method has been widely applied to the electrophysiological signal processing. However, the EMD method makes it difficult to calculate the exact within-frequency information of signals because the IMFs from different time series may correspond to different frequency bands. In order to remove this limitation, the EMD method was extended to the MEMD method which can simultaneously decompose multichannel of signals into

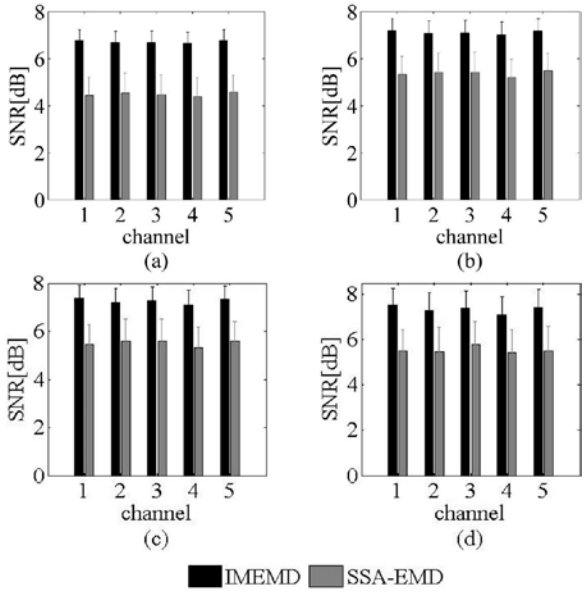

Fig. 6. The SNR differences between the IMEMD method and the SSA-EMD method after performing EOAs removal. The SNRs of the original artifact-contaminated EEG signals are -15dB (a), -10dB (b), -5dB (c), and 0dB (d). Mean values corresponding to different methods are represented by different color bars. Short bars: standard deviations.

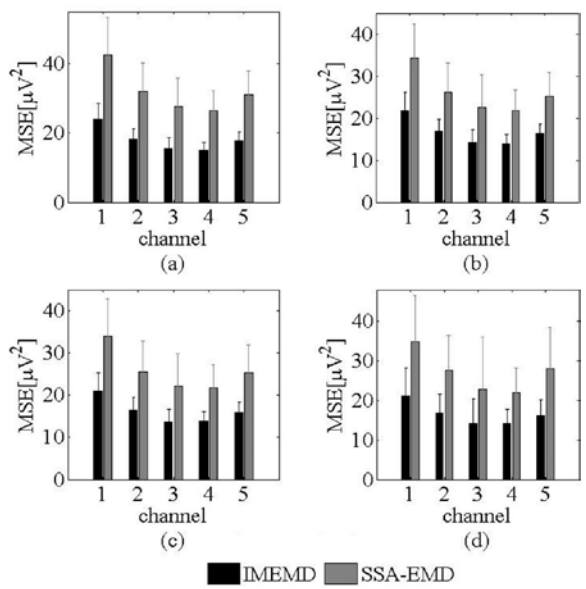

Fig. 7. The MSE differences between the IMEMD method and the SSA-EMD method after performing EOAs removal. The SNRs of original artifact-contaminated EEG signals are -15dB (a), -10dB (b), -5dB (c), and 0dB (d). Mean values corresponding to different methods are represented by different color bars. Short bars: standard deviations.

multiple paired IMFs within the same frequency bands [20]. Therefore, the IMEMD method could outperform the SSA-EMD technique.

V. CONCLUSION

In this study, the IMEMD method was proposed to remove EOAs from artifact-contaminated EEG signals. The performance of the proposed method was evaluated by simulated and real EEG signals. The simulation results indicated that the proposed method could successfully eliminate EOAs from simulated EEG signals and preserve useful EEG information with little loss. In addition, because the IMEMD based on maximum likelihood (ML) algorithm was superior to other three methods, this method was applied to removing EOAs from real EEG signals. There were significant differences between the CRC values before and after EOAs removal, which demonstrated that the EOAs have been well removed from real EEG signals. In comparison with other existing techniques, the proposed method achieved higher SNR and lower MSE than the AWICA and the SSA-EMD.

REFERENCES

[1] Y. Lingling, H. Leung, M. Plank, J. Snider, and H. Poizner, "EEG Activity During Movement Planning Encodes Upcoming Peak Speed and Acceleration and Improves the Accuracy in Predicting Hand Kinematics," *IEEE Journal of Biomedical and Health Informatics*, vol. 19, no. 1, pp. 22-28, 2015.

[2] P. Horki, D. S. Klobassa, C. Pokorny, and G. R. Muller-Putz, "Evaluation of Healthy EEG Responses for Spelling Through Listener-Assisted Scanning," *IEEE Journal of Biomedical and Health Informatics*, vol. 19, no. 1, pp. 29-36, 2015.

[3] G. Wang, G. Worrell, L. Yang, C. Wilke, and B. He, "Interictal spike analysis of high-density EEG in patients with partial epilepsy," *Clin Neurophysiol*, vol. 122, no. 6, pp. 1098-105, Jun, 2011.

[4] V. Mihajlovic, B. Grundlehner, R. Vullers, and J. Penders, "Wearable, Wireless EEG Solutions in Daily Life Applications: What are we Missing?," *Biomedical and Health Informatics, IEEE Journal of*, vol. 19, no. 1, pp. 6-21, 2015.

[5] Q. Zhao, B. Hu, Y. Shi, Y. Li, P. Moore, M. Sun, and H. Peng, "Automatic identification and removal of ocular artifacts in EEG--improved adaptive predictor filtering for portable applications," *IEEE Trans Nanobioscience*, vol. 13, no. 2, pp. 109-17, Jun, 2014.

[6] L. Shoker, S. Sanei, W. Wang, and J. A. Chambers, "Removal of eye blinking artifact from the electro-encephalogram, incorporating a new constrained blind source separation algorithm," *Med Biol Eng Comput*, vol. 43, no. 2, pp. 290-5, Mar, 2005.

[7] J. L. Kenemans, P. C. Molenaar, M. N. Verbaten, and J. L. Slangen, "Removal of the ocular artifact from the EEG: a comparison of time and frequency domain methods with simulated and real data," *Psychophysiology*, vol. 28, no. 1, pp. 114-21, Jan, 1991.

[8] T. P. Jung, S. Makeig, M. Westerfield, J. Townsend, E. Courchesne, and T. J. Sejnowski, "Removal of eye activity artifacts from visual event-related potentials in normal and clinical subjects," *Clin Neurophysiol*, vol. 111, no. 10, pp. 1745-58, Oct, 2000.

[9] J. W. Kelly, D. P. Siewiorek, A. Smailagic, J. L. Collinger, D. J. Weber, and W. Wang, "Fully automated reduction of ocular artifacts in high-dimensional neural data," *IEEE Trans Biomed Eng*, vol. 58, no. 3, pp. 598-606, Mar, 2011.

[10] H. Peng, B. Hu, Q. Shi, M. Ratcliffe, Q. Zhao, Y. Qi, and G. Gao, "Removal of ocular artifacts in EEG--an improved approach combining DWT and ANC for portable applications," *IEEE J Biomed Health Inform*, vol. 17, no. 3, pp. 600-7, May, 2013.

[11] N. P. Castellanos, and V. A. Makarov, "Recovering EEG brain signals: Artifact suppression with wavelet enhanced independent component analysis," *Journal of Neuroscience Methods*, vol. 158, no. 2, pp. 300-312, 2006.

[12] N. Mammone, F. La Foresta, and F. C. Morabito, "Automatic Artifact Rejection From Multichannel Scalp EEG by Wavelet ICA," *IEEE Sensors Journal*, vol. 12, no. 3, pp. 533-542, 2012.

[13] R. Mahajan, and B. I. Morshed, "Unsupervised eye blink artifact denoising of EEG data with modified multiscale sample entropy, Kurtosis, and wavelet-ICA," *IEEE J Biomed Health Inform*, vol. 19, no. 1, pp. 158-65, Jan, 2015.

[14] N. E. Huang, Z. Shen, S. R. Long, M. L. C. Wu, H. H. Shih, Q. N. Zheng, N. C. Yen, C. C. Tung, and H. H. Liu, "The empirical mode decomposition and the Hilbert spectrum for nonlinear and non-stationary time series analysis," *Proceedings of the Royal Society a-Mathematical Physical and Engineering Sciences*, vol. 454, no. 1971, pp. 903-995, Mar 8, 1998.

[15] F. Marzbanrad, Y. Kimura, K. Funamoto, R. Sugibayashi, M. Endo, T. Ito, M. Palaniswami, and A. H. Khandoker, "Automated Estimation of Fetal Cardiac Timing Events From Doppler Ultrasound Signal Using Hybrid Models," *IEEE Journal of Biomedical and Health Informatics*, vol. 18, no. 4, pp. 1169-1177, 2014.

[16] L. Shing-Hong, C. Kang-Ming, and C. Da-Chuan, "The Progression of Muscle Fatigue During Exercise Estimation With the Aid of High-Frequency Component Parameters Derived From Ensemble Empirical Mode Decomposition," *IEEE Journal of Biomedical and Health Informatics*, vol. 18, no. 5, pp. 1647-1658, 2014.

[17] J. P. Lindsen, and J. Bhattacharya, "Correction of blink artifacts using independent component analysis and empirical mode decomposition," *Psychophysiology*, vol. 47, no. 5, pp. 955-60, Sep, 2010.

[18] H. Zeng, A. Song, R. Yan, and H. Qin, "EOG artifact correction from EEG recording using stationary subspace analysis and empirical mode decomposition," *Sensors*, vol. 13, no. 11, pp. 14839-59, 2013.

[19] M. K. I. Molla, T. Tanaka, and T. M. Rutkowski, "Multivariate EMD based approach to EOG artifacts separation from EEG," in 2012 IEEE International Conference on Acoustics, Speech and Signal Processing (ICASSP), Kyoto, Japan, 2012, pp. 653-656.

[20] N. Rehman, and D. P. Mandic, "Multivariate empirical mode decomposition," *Proceedings of the Royal Society a-Mathematical Physical and Engineering Sciences*, vol. 466, no. 2117, pp. 1291-1302, May 8, 2010.

[21] P. Comon, "Independent Component Analysis, a New Concept?," *Signal Processing*, vol. 36, no. 3, pp. 287-314, Apr, 1994.

[22] A. Delorme, T. Sejnowski, and S. Makeig, "Enhanced detection of artifacts in EEG data using higher-order statistics and independent component analysis," *Neuroimage*, vol. 34, no. 4, pp. 1443-1449, Feb 15, 2007.

[23] G. Barbati, C. Porcaro, F. Zappasodi, P. M. Rossini, and F. Tecchio, "Optimization of an independent component analysis approach for artifact identification and removal in magnetoencephalographic signals," *Clin Neurophysiol*, vol. 115, no. 5, pp. 1220-32, May, 2004.

[24] S. Romero, M. A. Mananas, and M. J. Barbanoj, "A comparative study of automatic techniques for ocular artifact reduction in spontaneous EEG signals based on clinical target variables: a simulation case," *Comput Biol Med*, vol. 38, no. 3, pp. 348-60, Mar, 2008.

[25] S. H. Sardouie, M. B. Shamsollahi, L. Albera, and I. Merlet, "Denoising of Ictal EEG Data Using Semi-Blind Source Separation Methods Based on Time-Frequency Priors," *IEEE Journal of Biomedical and Health Informatics*, vol. 19, no. 3, pp. 839-847, 2015.

[26] A. Flexer, H. Bauer, J. Pripfl, and G. Dorffner, "Using ICA for removal of ocular artifacts in EEG recorded from blind subjects," *Neural Networks*, vol. 18, no. 7, pp. 998-1005, Sep., 2005.

[27] N. Yeung, R. Bogacz, C. B. Holroyd, and J. D. Cohen, "Detection of synchronized oscillations in the electroencephalogram: an evaluation of methods," *Psychophysiology*, vol. 41, no. 6, pp. 822-32, Nov, 2004.

[28] N. Yeung, R. Bogacz, C. B. Holroyd, S. Nieuwenhuis, and J. D. Cohen, "Theta phase resetting and the error-related negativity," *Psychophysiology*, vol. 44, no. 1, pp. 39-49, Jan, 2007.

[29] J. Gao, C. Zheng, and P. Wang, "Online removal of muscle artifact from electroencephalogram signals based on canonical correlation analysis," *Clin EEG Neurosci*, vol. 41, no. 1, pp. 53-9, Jan, 2010.

[30] G. Wang, Z. Wang, W. Chen, and J. Zhuang, "Classification of surface EMG signals using optimal wavelet packet method based on Davies-Bouldin criterion.," *Med Biol Eng Comput*, vol. 44, no. 10, pp. 865-72, Oct, 2006.

[31] N. Millor, P. Lecumberri, M. Gomez, A. Martinez-Ramirez, and M. Izquierdo, "Drift-free position estimation for periodic movements using inertial units," *IEEE J Biomed Health Inform*, vol. 18, no. 4, pp. 1131-7, Jul, 2014.

[32] C. Park, D. Looney, N. U. Rehman, A. Ahrabian, and D. P. Mandic, "Classification of Motor Imagery BCI Using Multivariate Empirical Mode Decomposition," *IEEE Transactions on Neural Systems and Rehabilitation Engineering*, vol. 21, no. 1, pp. 10-22, Jan, 2013.